The Journal of Immunology

Advanced Intercross Line Mapping of *Eae5* Reveals *Ncf-1* and *CLDN4* as Candidate Genes for Experimental Autoimmune Encephalomyelitis

Kristina Becanovic, Maja Jagodic, Jian Rong Sheng, Ingrid Dahlman, Fahmy Aboul-Enein, Erik Wallstrom, Peter Olofsson, Rikard Holmdahl, Hans Lassmann and Tomas Olsson

J Immunol 2006; 176:6055-6064; ;
doi: 10.4049/jimmunol.176.10.6055
http://www.jimmunol.org/content/176/10/6055

The Journal of Immunology is published twice each month by
The American Association of Immunologists, Inc.,
1451 Rockville Pike, Suite 650, Rockville, MD 20852

Print ISSN: 0022-1767 Online ISSN: 1550-6606.

Advanced Intercross Line Mapping of *Eae5* Reveals *Ncf-1* and *CLDN4* as Candidate Genes for Experimental Autoimmune Encephalomyelitis[1]

Kristina Becanovic,[2]* Maja Jagodic,* Jian Rong Sheng,* Ingrid Dahlman,* Fahmy Aboul-Enein,† Erik Wallstrom,* Peter Olofsson,‡ Rikard Holmdahl,‡ Hans Lassmann,† and Tomas Olsson*

Eae5 **in rats was originally identified in two F_2 intercrosses, (DA × BN) and (E3 × DA), displaying linkage to CNS inflammation and disease severity in experimental autoimmune encephalomyelitis (EAE), respectively. This region overlaps with an arthritis locus, *Pia4*, which was also identified in the (E3 × DA) cross. Two congenic strains, BN.DA-*Eae5* and BN.DA-*Eae5*.R1, encompassing the previously described *Eae5* and *Pia4,* were established. DA alleles within the chromosome 12 fragment conferred an increase in disease susceptibility as well as increased inflammation and demyelination in the CNS as compared with BN alleles. To enable a more precise fine mapping of EAE regulatory genes, we used a rat advanced intercross line between the EAE-susceptible DA strain and the EAE-resistant PVG.1AV1 strain. Linkage analysis performed in the advanced intercross line considerably narrowed down the myelin oligodendrocyte glycoprotein-EAE regulatory locus (*Eae5*) to a ~1.3-megabase region with a defined number of candidate genes. In this study we demonstrate a regulatory effect of *Eae5* on MOG-EAE by using both congenic strains as well as fine mapping these effects to a region containing *Ncf-1*, a gene associated with arthritis. In addition to structural polymorphisms in *Ncf-1*, both sequence polymorphisms and expression differences were identified in *CLDN4*. CLDN4 is a tight junction protein involved in blood-brain barrier integrity. In conclusion, our data strongly suggests *Ncf-1* to be a gene shared between two organ-specific inflammatory diseases with a possible contribution by *CLDN4* in encephalomyelitis.** ***The Journal of Immunology,*** **2006, 176: 6055–6064.**

Multiple sclerosis (MS)[3] is a chronic inflammatory and demyelinating disease of the CNS causing neurological deficits. There is evidence for a genetic predisposition to develop MS with a λ_{sib} value of 20–40 (1). Although the HLA region has proven to be associated with MS (2–5), it has turned out to be difficult to link distinct genes to MS susceptibility in both family linkage studies and association studies. This difficulty could be attributed to genetic heterogeneity, modest or weak effects of each disease-predisposing gene, and insufficient sample sizes. Rodent animal models of MS such as experimental autoimmune encephalomyelitis (EAE) reduce these problems, because analysis can be conducted in large crosses of EAE-resistant and EAE-susceptible inbred strains. Genome-wide linkage analysis has identified several loci linked to susceptibility in the mouse and rat (6–15). These loci are still large, encompassing hundreds of genes. Demonstration of the biological effect of an EAE-regulating quantitative trait locus (QTL) requires analysis of congenic strains, and further exact positioning requires extensive breeding to isolate the disease-regulating genes. A shortcut to further narrow the confidence intervals within the QTLs can be achieved by using an advanced intercross line (AIL) in which F_2 rats are intercrossed for additional generations. This narrowing is due to an accumulated increase in the number of recombinations compared with an F_2 intercross (16). In addition, the AIL may allow calculations of epistatic interactions within QTLs, in contrast to congenic mapping in which such interactions are difficult to identify systematically. We here combine congenic strains and an AIL to study *Eae5*. This locus is of interest for two reasons: 1) it displays linkage to CNS inflammation in an F_2 (DA × BN) cross (9) and linkage to EAE severity in an F2 (E3 × DA) cross (14); and 2) it overlaps with an arthritis-regulating locus, *Pia4* (17), in which we recently positionally cloned a major contributing gene, *Ncf-1* (18).

We use EAE induced with myelin oligodendrocyte glycoprotein (MOG) because, compared with many other rodent models, it displays a chronic relapsing disease course, demyelination, and axonal damage more closely resembling human MS (19–21). In addition, similar to MS but unlike most EAE models, there appears to be a pathogenic role of demyelinating Abs in MOG-EAE (22–24). To define the underlying genes in the *Eae5* locus we took advantage of both congenic strains and an AIL. A congenic strain,

*Department of Clinical Neuroscience, Neuroimmunology Unit, Karolinska Institutet, Stockholm, Sweden.; †Brain Research Institute, University of Vienna, Vienna, Austria; ‡Section for Medical Inflammation Research, Biomedical Center, Lund University, Lund, Sweden

Received for publication November 22, 2005. Accepted for publication February 27, 2006.

The costs of publication of this article were defrayed in part by the payment of page charges. This article must therefore be hereby marked *advertisement* in accordance with 18 U.S.C. Section 1734 solely to indicate this fact.

[1] This study was supported by a postdoctoral fellowship grant from the Swedish Brain Foundation, the Swedish Medical Research Council, European Union Biomed 2 Grant BMH 4-97-2027, the "Network for Inflammation Research" funded by the Swedish Foundation for Strategic Research, the Petrus and Augusta Hedlunds Foundation, the Swedish Foundation for the Neurologically Disabled, the Nils and Bibbi Jenssens Foundation, and the Montel Williams Foundation.

[2] Address correspondence and reprint requests to Dr. Kristina Becanovic, Karolinska Institutet, Department of Clinical Neuroscience, Section for Neuroscience Research, Neuroimmunology Unit, CMM L8:04, Karolinska Hospital, SE-171 76 Stockholm, Sweden, E-mail address: Kristina.Becanovic@cmm.ki.se

[3] Abbreviations used in this paper: MS, multiple sclerosis; AIL, advanced intercross line; EAE, experimental autoimmune encephalomyelitis; G7, seventh generation; LOD, base 10 logarithm of the likelihood ratio; Mb, megabase; MOG, myelin oligodendrocyte glycoprotein; p.i., post immunization; QTL, quantitative trait locus; SNP, single nucleotide polymorphism; UTR, untranslated region; Ct, cycle threshold.

0022-1767/06/$02.00

BN.DA-*Eae5*, was established through introgression of a chromosome 12 DA fragment into the resistant BN background. BN contains the MOG-EAE-susceptible RT.1N MHC haplotype (19, 25), although the non-MHC BN background genes provide a relative resistance (19). Congenic BN.DA-*Eae5* and the recombinant BN.DA-*Eae5*.R1, sharing a region on chromosome 12 inherited from DA, developed a more severe disease as compared with BN, confirming the original F_2 mapping data. To further confirm and localize *Eae5*, we used an advanced intercross line in the seventh generation (G7) in a cross between EA-susceptible DA and EA-resistant PVG.1AV1 rats (both of which share the same RT.1AV1 MHC haplotype). Fine mapping of the *Eae5* locus in the AIL confirmed the EAE association and limited the region to a ~1.3-megabase (Mb) region comprising only 20 genes. The mRNA from these genes was analyzed for both sequence and expression differences between DA, PVG.1AV1, and BN. Polymorphisms were identified in *Ncf-1*, and we here suggest it to be an example of a shared gene between different organ-specific inflammatory diseases in rat, i.e., EAE and experimental arthritis. Furthermore, both sequence and expression data suggest *CLDN4* as an additional modifier gene operating in encephalomyelitis. The syntenic region in human (7q11.23) has previously displayed suggestive linkage to MS (26). Accordingly, this comparative mapping approach suggests *CLDN4* as an obvious candidate to be tested in association studies using human MS material and healthy controls. Moreover, CLDN4 is a tight junction protein involved in the blood-brain barrier integrity (27), making it at this stage already an interesting candidate for drug targeting and for acting as a biomarker in MS.

Materials and Methods

Congenic rats

BN rats were originally obtained from the Zentralinstitut für Versuchstierzucht (Hannover, Germany) and commercially bought from Harlan. BN rats from Harlan were used in the second experiment performed. In the third experiment we used BN rats both from Harlan and from our own breeding, and we can confirm that there is no significant difference between the strains under the current experimental conditions (data not shown). To establish congenic BN.DA-*Eae5* rats, (BN × DA)F_1 rats were backcrossed for seven generations using the speed congenic approach (28). One hundred microsatellite markers were used to screen the genome background in the N4 rats. Rats with the least degree of DA alleles in the background genome were chosen for breeding. BN.DA-*Eae5* harbors DA alleles between D12Mgh1 and D12Rat22 (D12Rat22 is a telomeric marker) (38 cM fragment). BN.DA-*Eae5*.R1 harbors DA alleles in the interval, D12Mgh1-D12Rat26 (10 cM fragment) (see Fig. 1). BN.DA-*Eae5*.R1 is homozygous BN in D12Mgh5. We could only include four recombinant BN.DA-*Eae5*.R1 rats, because the breeding of this strain was very unproductive. All animals were kept locally in light- and temperature-regulated rooms under specific pathogen-free conditions (with free access to water and food). The North Stockholm Ethical Committee approved the experiments.

Advanced intercross line

The advanced intercross line was established from DA and PVG.1AV1 rats, both originally obtained from Zentralinstitut für Versuchstierzucht. To create the F_1 generation, two breeding pairs with DA as female founders and two breeding pairs with PVG.1AV1 as the female founder were bred. The F_2 generation was produced from seven pairs of F_1 rats with DA and PVG.1AV1 as female founders, respectively. The third generation originated from 50 breeding pairs with both types of female founders. Random breeding of 50 males and females produced all following generations, avoiding brother-sister mating throughout the breeding program. Finally, three G7 litters were produced for MOG-EAE experiments. The litters were similar in size, with almost equal numbers of females and males. One thousand sixty-eight G7 animals were selected for EAE experiments.

Induction and clinical evaluation of EAE

Rats between 8 and 11 wk of age were anesthetized with isoflurane (Abbott Laboratories) and immunized intradermally in the tail base. Each rat received 200 μl of inoculum containing recombinant MOG (aa 1–125) (29) in PBS (Invitrogen Life Technologies) emulsified 1:1 with IFA (Sigma-Aldrich). Two hundred micrograms of *Mycobacteria tuberculosis* (Difco Laboratories) was added to the described induction protocol for the experiments with congenic BN.DA-*Eae5* and BN.DA-*Eae5*.R1 and parental BN rats. Animals were weighed, and clinical signs of disease were evaluated from day 7 to days 30–35 postimmunization (p.i.). The signs were scored as follows: 1, tail weakness or tail paralysis; 2, hind leg paraparesis (gait disturbance) or hemiparesis; 3, hind leg paraparalysis or hemiparalysis; 4, tetraplegia with urinary and/or fecal incontinence; and 5, death and/or sacrifice due to severe EAE. If severe balance disturbance and/or severe disease was observed for more than 1 day, the rat was sacrificed. EAE score was defined when the rat displayed clinical signs for more than 1 day, and onset was calculated as the first day the clinical signs were observed. Rats that died before the day of sacrifice were included in the scoring with an EAE score of 5. This was done to prevent a reduction in power of the statistical analysis. Balance disturbance was scored as follows: 1, tilted walk; 2, severe leaning position; and 3, spinning. The experiment with BN and BN.DA-*Eae5* was repeated four times, and pooled data are displayed in Table I.

Histopathologogical evaluation

Rats from the first and second experiment performed were sacrificed and perfused via the left ventricle of the heart with 4% paraformaldehyde on day 30 p.i. Brains and spinal cords were dissected and embedded in paraffin wax. Sections 2- to 4-μm-thick were cut on a microtome and stained with H&E to assess inflammation and with Luxol fast blue and periodic acid-Schiff to assess demyelination (20). Inflammation and demyelination were assessed on brain and spinal cord sections. To assess the extent of inflammation, the mean number of inflammatory infiltrates around vessels in the spinal cord was evaluated. To assess the degree of demyelination, a semi-quantitative score slightly modified from that described by Storch et al. (20) was used. The scale ranged from 0 to 4 for brain and spinal cord, with a maximum score of 8 per animal. The scores were obtained as follows: 1, perivascular/subpial demyelination; 2, marked demyelination; 3, extended demyelination, e.g., more than half of the spinal cord white matter or one optic nerve or more than half of the cerebellar white matter; and 4, full demyelination of the spinal cord white matter, both optic nerves, or the cerebellar white matter.

Anti-MOG IgG-isotype determination

Serum was sampled from each rat day 14 p.i. We used ELISA to determine anti-MOG IgG, IgG1, IgG2a, IgG2b, and IgG2c for each rat. ELISA plates (Nunc) were coated with recombinant rat MOG (aa 1–125) diluted in 0.1 M $NaHCO_3$ (pH 8.2) at a concentration of 10 μg/ml. One hundred microliters of the MOG dilution was added to each well. The coated plates were stored overnight at 4°C. The sera for measuring IgG, IgG2a, and IgG2b

Table I. *Summary of the clinical EAE outcome in chromosome 12 congenic strains compared with BN*[a]

Strain	Incidence[b]	Mean Day of Onset ± SD[b]	Maximum Clinical EAE Score						Mean Maximum EAE Score ± SD[c]	Mean Cumulative Score ± SD[c,d]	Mortality
			0	1	2	3	4	>4			
BN	25/58	15.6 ± 3.9	33		6	8	1	10	1.55 ± 1.98	19.9 ± 31.8	9/58
BN.DA-*Eae5*	33/45**	14.6 ± 4.9	12	1	1	5	9	17	3.09 ± 2.08***	42.1 ± 33.9***	16/45*
BN.DA-*Eae5*.R1	4/4*	12.5 ± 0.6						4	5.0 ± 0**	83.3 ± 4.3**	4/4**

[a] The p values were calculated when comparing BN with BN.DA-*Eae5* and BN.DA-*Eae5*.R1, respectively, using with the Mann-Whitney *U* test; *, $p \leq 0.05$; **, $p \leq 0.01$; ***, $p \leq 0.001$.
[b] Incidence indicates affected animals/total number of animals.
[c] Mean values calculated include both affected and unaffected animals, except for day of onset where mean value only includes affected rats.
[d] Rats that died before day of sacrifice were calculated with EAE score of 5 until days 30–35 p.i. for cumulative EAE score.

isotype levels were diluted 1/2500, 1/2000, and 1/2500, respectively, and the sera for IgG1 and IgG2c were diluted 1/250 and 1/200, respectively. Antisera were diluted as follows: 1/2000 for IgG, IgG2a, and IgG2b; 1/1000 for IgG1; and 1/500 for IgG2c (Nordic). Goat anti-rabbit conjugate was diluted 1/10,000 (Nordic). OD values were read at 450 nm. Each plate had DA serum (immunized with MOG) as a positive control in duplicate. Arbitrary units were calculated for each rat and for each IgG isotype by comparing the values with the standard curve of the positive control for each ELISA plate.

Genotype analysis

Genomic DNA was prepared from tail tips according to a standard protocol (30). Microsatellite markers polymorphic for the DA and PVG.1AV1 strains were used for PCR-based amplification together with primers end labeled with [γ-^{33}P]ATP (31). Primers were obtained from Genset. PCR products were size fractionated on 6% polyacrylamide gels and visualized by autoradiography. Single nucleotide polymorphism (SNP) markers that distinguish between DA and PVG.1AV1 in the coding region of *Ncf-1* were produced previously (18). Polymorphisms were identified by sequencing at nt 330 (A in DA and BN and G in PVG.1AV1) and nt 472 (T in DA and C in BN and PVG.1AV1). Genotype analyses for the SNP markers in exon 4 and 6 in *Ncf-1* were run using the Pyrosequencing PSQ 96 system according to protocols supplied by the manufacturer (Biotage).

Relative quantification of mRNA by real-time quantitative PCR

Tissue samples from thymus, spleen, lymph node, brain (hippocampal level), and spinal cord (cervical level) were sampled from naive and MOG-immunized DA, PVG.1AV1, and BN rats, respectively. Tissues were sampled on the day of EAE onset in the MOG-immunized rats. Sampling of a diseased DA rat resulted in the same sample number of PVG.1AV1 and BN rats, respectively. These tissues were considered to be of biological importance in EAE. Cells for each tissue were lysed, and total RNA was extracted (Qiagen total RNA extraction kit). Samples were incubated with DNase according to the manufacturer's protocol (Qiagen; RNase-free DNase set) for 30 min at room temperature to avoid amplification of contaminating genomic DNA. Reverse transcription was performed with 10 μl of total RNA, random hexamer primer (0.1 μg; Invitrogen Life Technologies), and SuperScript reverse transcriptase (200 U; Invitrogen Life Technologies). Quantitative analyses of mRNA expression were performed using QuantiTect SYBR Green according to the manufacturer's instructions (Qiagen). Amplification was performed using an ABI PRISM 7700 sequence detection system (PerkinElmer). All primers were designed using the Primer Express software (PerkinElmer). Primers were constructed over exon/exon boundaries to avoid amplification of contaminating genomic DNA. Relative quantification of mRNA levels was calculated using the standard curve method, with amplification of mRNA and GAPDH in separate tubes (as described in PerkinElmer Applied Biosystems User Bulletin No. 2, ABI PRISM 7700 Sequence Detection System; December 11, 1997). Standard curves were created using four serial dilutions (1/1, 1/10, 1/100, and 1/1000) of liver cDNA equally mixed from five MOG-immunized DA and five MOG-immunized PVG.1AV1 rats. Each sample was run in duplicate with primers for GAPDH and the different target mRNA, respectively, in different wells. Samples without added cDNA served as negative controls. The relative amount of mRNA in each well was calculated as the ratio between the target mRNA and the endogenous GAPDH. ΔCt, i.e., Ct value for target $-$ Ct value for *GAPDH* (where Ct is cycle threshold), was calculated for *WBSCR28*. The first experiment was performed on brain tissue in naive DA ($n = 4$) and PVG.1AV1 rats ($n = 4$). The second experiment included naive and MOG-immunized DA and PVG.1AV1 rats, respectively. We analyzed tissue from thymus, spleen, lymph node, brain, and spinal cord in pooled groups of naive DA ($n = 8$), naive PVG.1AV1 ($n = 8$), MOG-immunized DA ($n = 5$), and MOG-immunized PVG.1AV1 ($n = 8$) rats. All 20 genes within the confidence interval of *Eae5* were analyzed. Subsequently, we quantified the expression of *CLDN4* individually in spleen, lymph node, brain, and spinal cord in individual samples of naive and MOG-immunized DA, PVG.1AV1, and BN rats (naive DA, $n = 8$; naive PVG.1AV1, $n = 8$; naive BN, $n = 7$; MOG-immunized DA, $n = 5$; MOG-immunized PVG.1AV1, $n = 8$; and MOG-immunized BN, $n = 8$). *Tri50* and *FKBP6* were not expressed.

Sequence analysis

Primers for the sequencing of each target gene were designed using the Oligo 6.0 version software (National Biosciences). Genomic DNA from DA and PVG.1AV1 was used as source for sequencing of *NSUN5*, *Tri50*, *FKBP6*, *Fzd9*, *BAZ1B*, *CLDN4*, *WBSCR27*, *WBSCR28*, *Eln*, *Limk1*, *WBSCR1*, *Wbscr5*, *RFC2*, *Cyln2*, *GTF2IRD1*, *GTF2I*, *Ncf-1*, *GTF2IRD2*, *WBSCR16*, and *GATS* in combination with cDNA for *NSUN5* (liver), *Fzd9* (brain), *BAZ1B* (liver), *WBSCR27* (liver), *Eln* (liver), *Limk1* (brain), *WBSCR1* (liver), *RFC2* (liver), *Cyln2* (brain), *GTF2IRD1* (liver), *GTF2I* (liver), *Ncf-1* (liver), *GTF2IRD2* (liver), *WBSCR16* (brain), *and GATS* (brain). Tissue source is indicated in parentheses and was chosen upon evaluation of degree of expression when comparing brain, liver, spleen, and kidney in DA rat. PCR were performed according to conventional protocols and/or using the Advantage 2 PCR kit according to protocols supplied by the manufacturer for sequences longer than 2 kb (BD Clontech). All PCR products were run separately on 0.8–2% agarose gels for evaluation of the size of the PCR product. Sequencing reactions were performed using Mix v3.1 Big Dye according to protocols supplied by the manufacturer (Applied Biosystems).

Statistical analysis

The Mann-Whitney *U* test was used to compare the clinical scores, anti-MOG IgG levels, inflammation index, and demyelination for BN, BN.DA-*Eae5*, and BN.DA-*Eae5*.R1 rats. Fisher's exact test was used to analyze whether there was a difference in observed genotype distribution between affected rats, i.e., rats with positive clinical scores, and nonaffected rats. In addition, the Kruskal-Wallis ranking test was used to determine whether different genotypes in the AIL were associated with differences in maximum EAE score, cumulative EAE score, weight loss, demyelination, inflammation, and anti-MOG Ab levels. All of the statistical analyses mentioned above were performed using JMP version 5.0 (SAS Institute). MAPMAKER/EXP version 3.0 (32) was used to create a genetic map, and linkage analysis was performed using the MAPMAKER/QTL (32). The confidence interval was arbitrarily defined as a drop in a base 10 logarithm of the likelihood ratio (LOD) of 1. The linkage analysis was confirmed using R/qtl software (33). Permutation analysis was performed to determine the significance levels based on the analyzed sample material (34, 35). Permutation analysis involves repeated shuffling of the trait values 1000 times among the genotypes to calculate relevant significance levels. The permutation procedure based on the investigated material is empirical and reflects the characteristics of the particular trait to which it is applied. This method does not rely on distributional assumptions regarding the quantitative trait and is valid in a small sample (35). We present the thresholds obtained for highly significant linkage in *Results*. For calculation of linkage to the following phenotypes, we used the methods given in parentheses: incidence of EAE (nonparametric model); maximum EAE score, (Haley-Knott regression); cumulative EAE score and duration of EAE (two-part model). The following maximum LOD values were obtained: LOD of 4.2 for incidence of EAE (LOD score corresponding to $p = 0.001$ is 2.9); LOD of 5.0 for maximum EAE score (LOD score corresponding to $p = 0.001$ is 3.1); LOD of 5.7 for cumulative EAE score (LOD score corresponding to $p = 0.001$ is 3.5); LOD of 7 for duration of disease (LOD score corresponding to $p = 0.001$ is 3.8)

Results

Clinical EAE parameters

The parental DA strain displays a severe relapse-remitting disease course, with disease onset on average 2 wk after immunization,

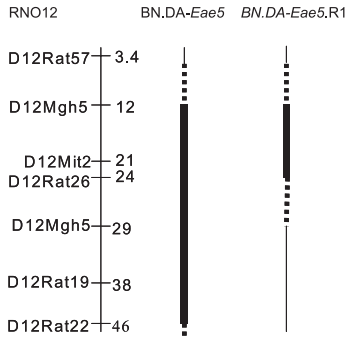

FIGURE 1. Genetic map of rat chromosome 12 (RNO12) aligned with congenic intervals in BN.DA-*Eae5* and BN.DA-*Eae5*.R1, respectively. The RNO12 map contains microsatellite markers used for congenic breeding and for definition of their borders. Microsatellite marker positions were placed according to a relative scale based on genome sequence retrieved from Ensembl. Thick vertical lines indicate the congenic fragment with homozygous DA alleles on a BN background (thin line). Dotted lines indicate recombination sites.

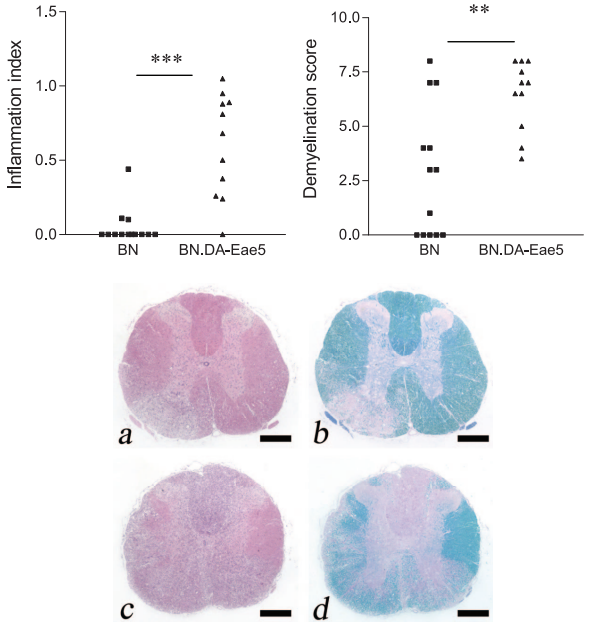

FIGURE 2. Inflammation and demyelination assessed by histopathological evaluation of brain and spinal cord sections at day 30 p.i. The *left* and the *right scatter plots* demonstrate the mean number of inflammatory infiltrates around vessels in the spinal cord and the degree of demyelination between BN and BN.DA-*Eae5,* respectively. All BN.DA-*Eae5* rats displayed demyelination. Ten of eleven BN.DA-*Eae5* rats also displayed severe clinical EAE. BN rats displayed a more variable histopathological and clinical correlation, with equal numbers of rats displaying no EAE and no histopathological phenotypes, no clinical EAE but some degree of demyelination, and clinical EAE along with demyelination and/or inflammation. BN.DA-*Eae5* displayed a higher degree of inflammation ($p = 0.0002$, Mann-Whitney *U* test) as well as demyelination ($p = 0.006$) compared with BN (*, $p \leq 0.05$; **, $p \leq 0.01$; ***, $p \leq 0.001$). Histopathological analysis of spinal cords of representative animals (medians of each strain) of BN and BN.DA-*Eae5* are shown in the lower portion of the figure, where *a* and *b* represent BN and *c* and *d* represent BN.DA-*Eae5.* Analysis showed clear differences in the numbers of infiltrating immune cells (*a* and *c*, hematoxylin) as well as extent of demyelination (*b* and *d*, Luxol fast blue) in experimentally induced CNS inflammation. Scale bars, 150 μm

whereas the BN strain displayed a moderate incidence rate with our immunization protocol (Table I). The EAE effect in BN is reminiscent of an on/off effect, where diseased BN usually displayed severe EAE with a chronic progressive disease course. Nevertheless, we could detect significant differences between the BN and the congenic BN.DA-*Eae5* (38 cM) for several of the EAE phenotypes, i.e., incidence of EAE, maximum EAE score, cumulative EAE score, and mortality (Table I) (Fig. 1). We also tested a rat strain with a smaller congenic fragment i.e., BN.DA-*Eae5*.R1 (10 cM), which developed very severe and chronic EAE compared with BN (Fig. 1).

Eae5 is associated with increased inflammation and demyelination

The degree of inflammation and demyelination was assessed in brain and spinal cord sections day 30 p.i. (Fig. 2, *a–d*). These phenotypes were distributed in a similar way as the clinical signs of disease. Ten of the eleven BN.DA-*Eae5* rats displayed severe clinical EAE, whereas all of them had both inflammation and demyelination in the CNS. In comparison, 8 of 13 BN rats displayed no EAE and no ($n = 4$) or a very low degree of demyelination ($n = 4$). One BN rat displayed maximum EAE score of 2 (only two days), but no demyelination or inflammation in the CNS. BN.DA-*Eae5* ($n = 11$) rats displayed a higher degree of inflammation ($p = 0.0002$, Mann-Whitney *U* test) as well as demyelination ($p = 0.006$) compared with the BN rats. The inflammation indices were relatively low compared with the demyelination scores, most apparent among BN rats. This result is expected in view of the late sampling in this study at day 30 p.i., a time point at which T cell and macrophage infiltration had decreased as compared with earlier in the disease course. One BN.DA-*Eae5* and four BN rats displayed histopathological but no clinical signs, suggesting a subclinical healed disease with histological sequelae, a subclinical active disease process, and/or signs not assessed in our scoring procedure such as sensory deficits.

Eae5 is associated with total serum Ab levels and anti-MOG-specific IgG2b antibodies

We measured anti-MOG Ab serum levels day 14 p.i. (Fig. 3). In addition, we measured anti-MOG IgG isotypes, which could potentially discriminate between a T1/T2 bias in the immune response. IgG2b and IgG2c are associated with T1 and IgG1 is associated with T2 responses in the rat (36) (37). We compared the anti-MOG Ab levels in BN ($n = 30$) and BN.DA-*Eae5* ($n = 28$) rats. BN.DA-*Eae5* rats displayed lower total anti-MOG IgG ($p = 0.014$, Mann-Whitney *U* test) and anti-MOG IgG2b ($p = 0.017$) isotype levels (Fig. 3). There was no significant difference in the anti-MOG IgG1, IgG2a, and IgG2c isotype levels.

SNP genotype data improved the level of significance at Eae5 by ~10-fold

We initially performed F_2 intercrosses to have enough power to identify QTLs regulating EAE (9, 14). These genome-wide scans

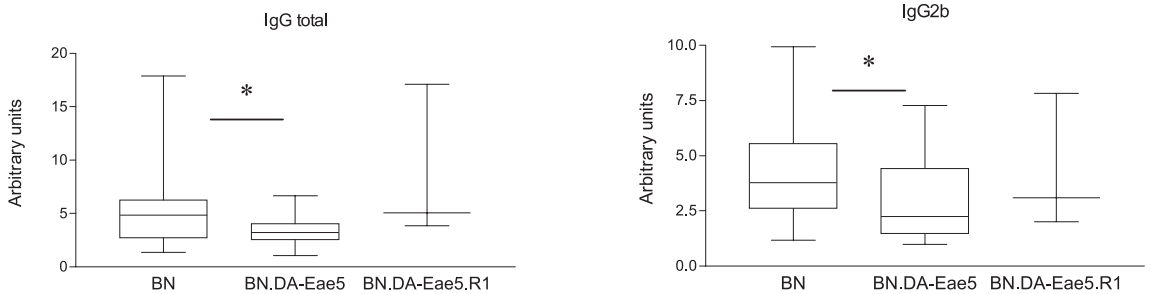

FIGURE 3. Anti-MOG Ab serum levels at day 14 p.i as measured by ELISA. BN.DA-*Eae5* ($n = 28$) rats displayed lower total IgG levels ($p = 0.014$; Mann-Whitney *U* test) and IgG2b isotype ($p = 0.017$) serum levels as compared with BN ($n = 30$). There were no differences in IgG1, IgG2a, and IgG2c isotype serum levels. BN.DA-*Eae5*.R1 ($n = 4$) did not show any differences in anti-MOG isotype levels as compared with BN. Data are presented in arbitrary units. The ends of the box plots show the 25th and 75th quartiles. The line across the middle of the box identifies the median sample value. The whiskers extend from the ends of the box to the outermost point. *, $p \leq 0.05$.

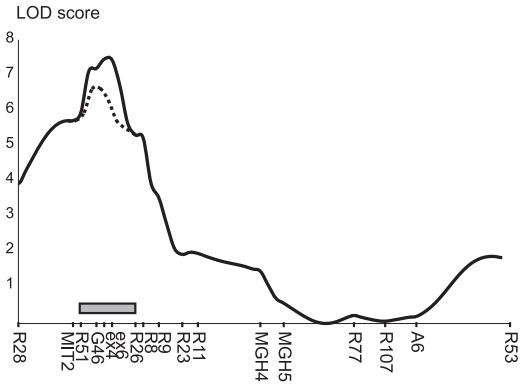

FIGURE 4. Log likelihood plots of *Eae5* using an G7 (DA × PVG.1AV1) intercross. The *y*-axis represents the LOD score, and the *x*-axis shows the microsatellite and SNP markers used in the genotype analysis (R, rat; G, Got; A, Arb; ex, exon). There is significant linkage to duration of disease (LOD = 7.5) shown in the figure, but there is also linkage to cumulative score (LOD = 5.8), EAE incidence (LOD = 4.3), and maximum EAE score (LOD = 5.6). Specific SNP markers in exon 4 and 6 in the *Ncf-1* gene were analyzed. The peak marker is in the *Ncf-1* exon 4 and exon 6 interval for all of the EAE phenotypes described. Linkage analysis was performed using MAPMAKER/QTL. The confidence interval encompasses seven confirmed genes and an additional thirteen unconfirmed genes in rat. The confirmed genes are *Tri50*, *Fzd9*, *Eln*, *Limk1*, *Wbscr5*, *Cyln2*, and *Ncf-1*. Genes within the interval described were retrieved from Ensembl version 29.

identified *Eae5* with a broad confidence interval. However, to enable a more precise fine mapping of EAE regulatory genes, we bred an AIL between the EAE-susceptible DA strain and the EA-resistant PVG.1AV1 strain. One thousand sixty-eight rats from this G7 population were subjected to MOG immunization and careful phenotyping for MOG-EAE as described earlier (30). Of 1068 MOG-immunized rats, 158 displayed clinical signs of EAE. We genotyped 152 (6 DNA samples were excluded due to poor quality) affected rats and a random selection of 162 unaffected rats with 15 microsatellite markers and 2 SNP markers dispersed over the *Eae5* locus on chromosome 12. There was significant linkage to duration of EAE (LOD = 7.5) with a peak over the *Ncf-1* locus (Fig. 4) and incidence of EAE (LOD = 4.3), maximum EAE score (LOD = 5.6), and cumulative EAE score (LOD = 5.8). Rats homozygous for DA alleles displayed a higher incidence of EAE and higher mean values for maximum EAE score, cumulative EAE score, and duration of EAE as compared with the other two genotype groups. There was no linkage to total anti-MOG IgG or isotype levels. Because the *Ncf-1* gene was found to explain the corresponding *Pia4* locus associated with arthritis (18), SNPs in exon 4 and 6 in the *Ncf-1* gene were also analyzed. Linkage analysis was performed before and after the addition of the *Ncf-1* SNP genotype data. SNP genotype data improved the significance at *Eae5* by ~10-fold (1 LOD unit) (Fig. 4). It is, however, important to note that a simple mapping model is not the optimal analysis for an AIL (i.e., its inability to account for randomization in breeding that obliterates cross structure in addition to fixation and correlation of genotypes between siblings). Currently, there are no analyses established that accurately account for these factors. The behavior of confidence intervals in AILs is thus not entirely clear, and our interval may be optimistically small. However, we consider the statistical significance of the peak to be a true finding, because the relevance of the *Ncf1* gene has been reported previously (38).

Table II. *Genes within the confidence interval of Eae5*

Gene[a,b]	Position in Rat	Possible Role in EAE
D12Rat51	22417925–22418145 bp (22.4 Mb)	
NSUN5	22439343–22444280 bp (22.4 Mb)	
Tri50	22446134–22461108 bp (22.4 Mb)	
FKBP6	22464623–22476654 bp (22.5 Mb)	Neuron survival and growth
Fzd9	22572493–22574271 bp (22.6 Mb)	
BAZ1B	22578825–22597102 bp (22.6 Mb)	Transcription factor
CLDN4	22687188–22687820 bp (22.7 Mb)	Tight junction protein, brain-blood barrier
WBSCR27	22693188–22701632 bp (22.7 Mb)	
WBSCR28	22730401–22734942 bp (22.7 Mb)	
Eln	22892483–22935863 bp (22.9 Mb)	
Limk1	22952110–22984673 bp (23.0 Mb)	CNS development
WBSCR1	23008919–23023902 bp (23.0 Mb)	Translation initiation factor
Wbscr5	23035111–23041465 bp (23.0 Mb)	
RFC2	23046412–23059175 bp (23.0 Mb)	
No description[c]	23072490–23073180 bp (23.1 Mb)	
No description[c]	23081041–23082885 bp (23.1 Mb)	
Cyln2	23088867–23152664 bp (23.1 Mb)	
GTF2IRD1	23181243–23289310 bp (23.2 Mb)	
D12Got46	23225514–23225729 bp (23.2 Mb)	
GTF2I	23350479–23408833 bp (23.4 Mb)	JAK in B cell signaling
Ncf-1	23441313–23449099 bp (23.4 Mb)	Subunit of NADPH oxidase complex
GTF2IRD2	23513696–23545170 bp (23.5 Mb)	
WBSCR16	23560961–23590301 bp (23.6 Mb)	
GATS	23600395–23637029 bp (23.6 Mb)	
D12Rat26	23708771–23708949 bp (23.7 Mb)	
D12Rat8	23797947–23798087 bp (23.8 Mb)	
D12Rat9	24333613–24333738 bp (24.3 Mb)	

[a] Genes confirmed in rat are written with a first capital letter and remaining letters in lowercase. Genes not confirmed, but with human and/or mouse orthologs, are written with capital letters. Microsattelite markers used within this region are indicated with bold letters and included at their respective positions. Data is retrieved from Ensembl version 29 (www.ensembl.org/Rattus_norvegicus/index.html.

[b] All genes are within the chromosomal location 12q12 in rat and 7q11.23 in human (Ensembl).

[c] Genes with no description were not analyzed.

Candidate genes within the Eae5 confidence interval

The 95% confidence interval from the linkage data was defined as a drop in LOD of 1 (39), and seven confirmed genes within this region and thirteen unconfirmed could be identified in this region (Fig. 4) (Table II). Two genes were annotated as unknown and did not have any orthologs in human or mouse. Among the 13 unconfirmed but predicted genes, all have orthologs in human and/or mouse, respectively. The confirmed genes are *Tri50*, *Fzd9*, *Eln*, *Limk1*, *Wbscr5*, *Cyln2*, and *Ncf-1*. This gene region is syntenic to human 7q11.23 (Ensembl; www.ensembl.org).

Defined polymorphisms and expression differences in a restricted set of genes

The expression analysis and sequencing of genes within the defined confidence interval of *Eae5* demonstrated a restricted number of differences when comparing DA, PVG.1AV1, and BN rats. The coding region of *NSUN5*, *Fzd9*, *BAZ1B*, *Wbscr5*, *GTF2IRD1*, and *GATS* contained polymorphisms between DA vs PVG.1AV1 and BN rats. These were, however, all synonymous and therefore unlikely to be of importance (Table III). Polymorphisms in the 3′ untranslated region (UTR) were detected when comparing sequences for *RFC2* and *GTF2I*. Furthermore, *Ncf-1* contained three polymorphisms where one SNP was synonymous (Arg), whereas two resulted in amino acid substitutions (M106V and M153T). This confirms earlier analysis showing that the only polymorphism of *Ncf-1* between DA, PVG.1AV1, and BN rats is the M153T substitution that is likely the disease-related mutation (40). The *GTF2IRD2* contained two polymorphisms, of which one was synonymous, whereas the other resulted in an A18S substitution. This SNP could be of relevance for protein structure and function. Quantification of mRNA expression for all genes within the confidence interval was performed (Fig. 5). We did not detect any consistent expression differences of *Ncf-1* between DA and PVG.1AV1, neither for the naive nor for the MOG-immunized samples analyzed (Fig. 5). Moreover, no differences were detected for *RFC2* and *GTF2I*. Therefore, SNPs in the UTR regions of *RFC2* and *GTF2I* probably do not influence gene expression. *CLDN4* contained a polymorphism resulting in a K191E substitution. This polymorphism segregated with EAE susceptibility in several rat strains, i.e., lysine, which is a basic acid in EAE-susceptible DA and LEW.1AV1 rats, and glutamic acid, which is an acidic amino acid in PVG.1AV1, BN, AC1, and E3 rats (Fig. 6*a*). Moreover, *CLDN4* was the only gene within *Eae5* displaying consistent expression differences detected between both naive and MOG-immunized DA and PVG.1AV1 rats (Fig. 5). Naive DA rats displayed lower expression of *CLDN4* in thymus, spleen, and lymph node as compared with naive PVG.1AV1 rats. MOG-immunized DA displayed even more distinct differences, with lower expression of *CLDN4* in thymus and spleen as well as brain and spinal cord as compared with PVG.1AV1 rats. This finding was further confirmed when analyzing *CLDN4* expression individually in naive and MOG-immunized DA, PVG.1AV1, and BN rats, respectively (Fig. 6*b*). DA expressed lower levels of *CLDN4* as compared with both PVG.1AV1 and BN. Thus, both expression and sequence data segregate with EAE susceptibility vs EAE resistance in the strains analyzed. There was a significant difference in *CLDN4* expression in spleen between EAE-susceptible DA and EAE-resistant PVG.1AV1 and BN rats (Fig. 6*b*). We cannot exclude the possibility that expression differences of specific genes in individual tissues may be of relevance at different time points during disease. Therefore, there are additional candidate genes within the confidence interval apart from *Ncf-1* that might influence EAE specifically. Of these, *CLDN4* is the most interesting.

Claudin orthologs in human and mice

The claudin gene identified in *Eae5* is not confirmed in rat but has claudin-3 and claudin-4 orthologs in both human and mouse. Sequence alignment analysis showed that the sequence homology to *Cldn4* in mouse was the highest (score 94), and the sequence homology to *Cldn3* in mouse and *Cldn3* and *Cldn4* in humans was

Table III. *Polymorphisms between DA, PVG.1AV1, and BN for genes within Eae5*

Gene[a,b]	SNP (bp)	Codon	DA[c]	PVG.1AV1[c]	BN[c,d]	Amino Acid Substitution[e]
NSUN5	36	12	GCG	**GCC**	**GCC**	Ala→Ala
Fzd9	1260	420	ACC	**ACA**	**ACA**	Thr→Thr
BAZ1B	1308	436	GTG	**GTT**	**GTT**	Val→Val
CLDN4[f]	571	191	AAA	**GAA**	**GAA**	Lys→Glu
Wbscr5	9	3	GCT	**GCC**	**GCC**	Ala→Ala
	168	56	**TCG**	TCA	**TCG**	Ser→Ser
RFC2	1088	3′ UTR	T	**C**	**C**$_r$	
GTF2IRD1	468	107	TGT	**TGC**	**TGC**	Cys→Cys
	930	261	TCA	**TCG**	**TCG**$_r$	Ser→Ser
GTF21	2992	3′ UTR	T	**C**	**C**	
Ncf-1	330	106	**ATG**	GTG	**ATG**$_r$	Met→Val
	472	153	ATG	**ACG**	**ACG**$_r$	Met→Thr
	1161	383	**AGG**	CGG	**AGG**$_r$	Arg→Arg
GTF2IRD2	53	18	GAC	**GGC**	**GGC**$_r$	Asp→Gly
	144	48	**GTA**	GTG	**GTA**	Val→Val
GATS	504	168	**CCT**	CCC	**CCT**	Pro→Pro
	780	260	**TCC**	TCT	**TCC**	Ser→Ser

[a] Table only includes the genes that contained polymorphisms between DA, PVG.1AV1, and BN. Genes confirmed in the rat are written with a first capital letter and remaining letters in lower case. Genes not confirmed but with orthologs in human and/or mouse are written with capital letters.

[b] Sequencing data does not include *Eln* exons 9–30 and *FKBP6* exon 2.

[c] Codons in boldface indicate identical codons between strains.

[d] Sequence for BN was obtained from locally bred BN or from reference sequence obtained from Ensembl (www.ensembl.org/Rattus_norvegicus/index.html) where **r** is indicated.

[e] Amino acid change due to gene polymorphisms. DA indicated to the left and PVG.1AV1 to the right of the arrow.

[f] *CLDN4* was sequenced in additional strains (LEW.1AV1 EAE-susceptible strain, and ACI and E3 EAE-resistant strains) and polymorphism at codon 191 was confirmed to segregate with disease *i.e.* AAA in DA, LEW.1AV1 and GAA in PVG.1AV1, BN, AC1, E3.

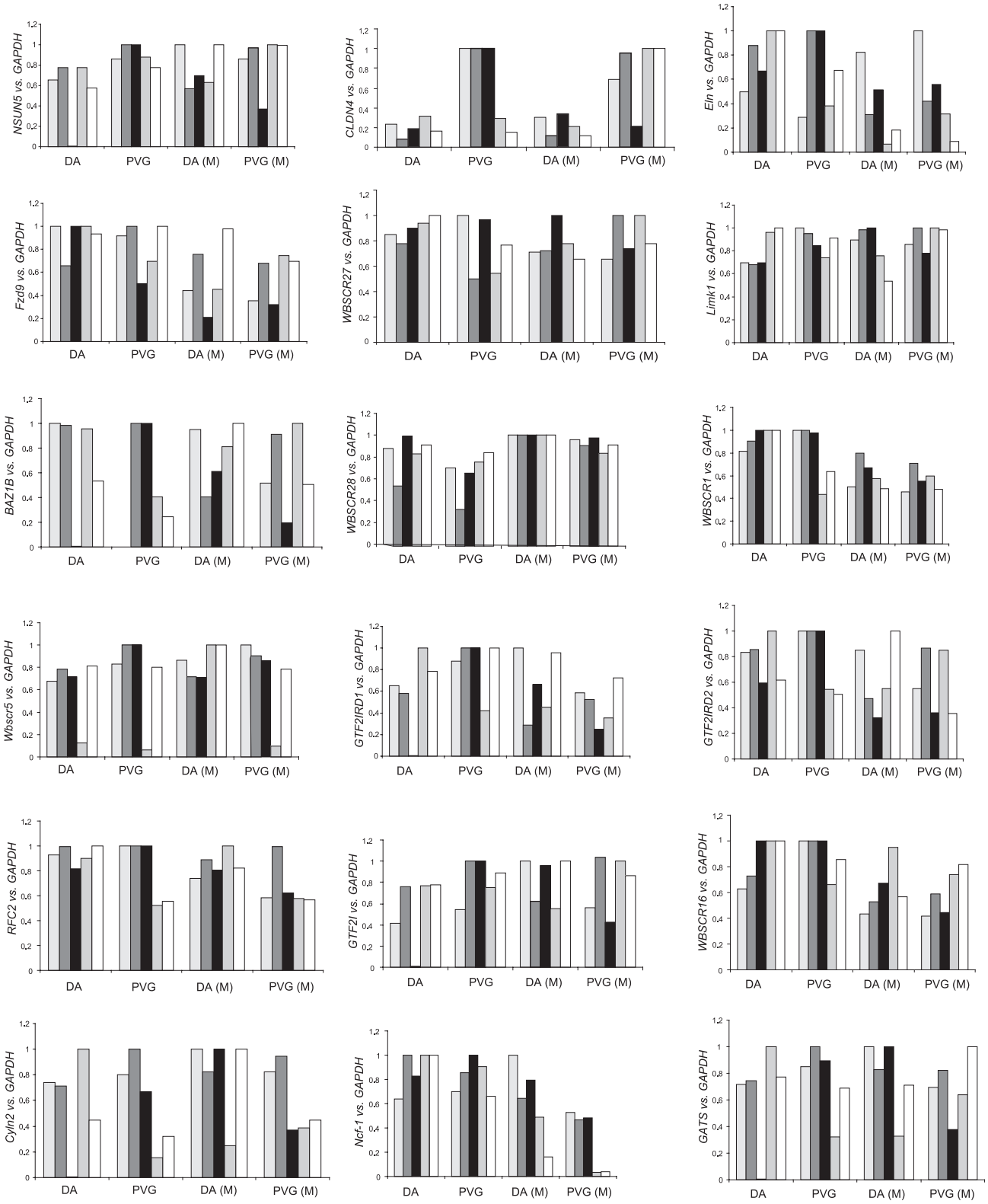

FIGURE 5. Quantification of the mRNA expression of genes in *Eae5*. Tissue samples from thymus (light gray), spleen (dark gray), lymph node (dark gray), spinal cord (gray) and brain (white) were pooled from naive DA ($n = 8$), naive PVG.1AV1 ($n = 8$), MOG-immunized (M) DA ($n = 5$), and MOG-immunized (M) PVG.1AV1 ($n = 8$). Relative quantification of mRNA levels was calculated using the standard curve method with amplification of mRNA and GAPDH. The relative amount of mRNA in each well was calculated as the ratio between the target mRNA and the endogenous GAPDH. ΔCt was calculated for *WB5CR28*.

the lowest (score between 65 and 84) (ClustalW; www.ebi.ac.uk/clustalw/index.html.). Both **Cldn3** and **Cldn4** play a major role in tight junctions. Tissue specificity and expression are, however, not well defined, because there is only information on high expression in lung and liver and lower expression in kidney and testis for both of these claudin genes (UniProt; www.ebi.uniprot.org/). However,

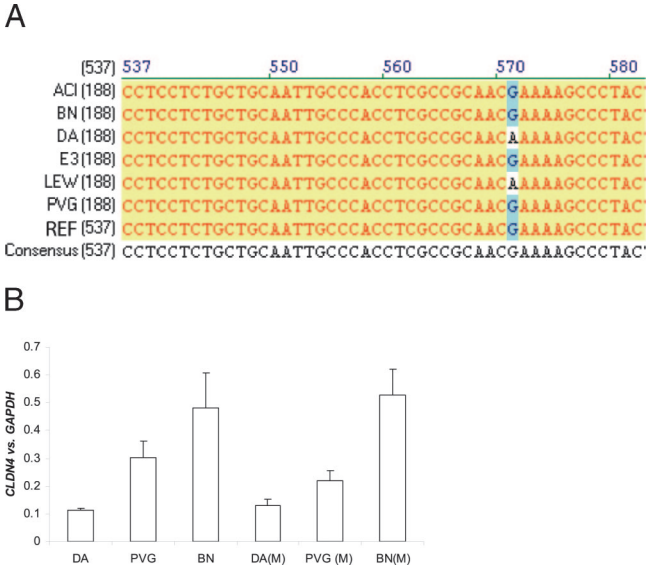

FIGURE 6. *a*, Sequencing of CLDN4 in EAE-susceptible and EAE-resistant strains. Sequencing analysis of several strains revealed a polymorphism resulting in a K191E substitution. This polymorphism segregated with EAE susceptibility in several rat strains, i.e., lysine, a basic amino acid in EAE-susceptible DA and LEW.1AV1 rats, and glutamic acid, an acidic amino acid in EAE-resistant PVG.1AV1, BN, AC1, and E3 rats. The reference sequence (REF) corresponds to the *CLDN4* sequence obtained from Ensembl. *b*, RT-PCR analysis of *CLDN4* transcript levels in spleen tissue sampled from naive and MOG-immunized (M) DA, PVG.1AV1, and BN rats, respectively. Tissue from MOG-immunized (M), EAE-susceptible DA rats was sampled on the individual day of EAE onset, together with the corresponding number of EAE-resistant PVG.1AV1 and BN rats, respectively. Naive PVG.1AV1 had significantly higher levels of *CLDN4* ($p < 0.05$) and tendencies in MOG-immunized PVG.1AV1 when compared with DA rats. Both naive ($p < 0.05$) and MOG-immunized ($p < 0.01$) BN rats displayed higher levels of *CLDN4* transcripts than DA rats. Error bars in the graph indicate the SEM.

it is of great relevance and importance to mention that it has previously been shown that expression of *Cldn3* is affected in brain during EAE in mouse (27). Furthermore, *Cldn1*, *Cldn2*, and *Cldn11* are expressed in mouse (41), and *Cldn5* is expressed in human brain (42). Mutations in *Cldn14* cause autosomal recessive deafness in humans and prove that defects in claudin genes are related to and cause human diseases (43).

Discussion

The results from the congenic strains demonstrate that DA alleles within *Eae5* are sufficient to aggravate EAE on a BN genome background, confirming previous findings in F_2 intercrosses (9, 17). The full-length congenic BN.DA-*Eae5* and the recombinant BN.DA-*Eae5*.R1, both with genome fragments that include the overlapping *Eae5* and *Pia4* (14), were more susceptible to EAE as compared with BN. This finding was consistent when comparing the clinical EAE course as well as the degree of demyelination and inflammation in the CNS. The total anti-MOG IgG Ab levels and the IgG2b isotype levels were lower in BN.DA-*Eae5* rats compared with BN rats (Fig. 3). The effects of the DA congenic fragment on anti-MOG IgG levels are, however, not interpretable in any simplistic way. In a broad sense they may reflect the effects on immunoregulation by genes in the fragment. Another explanation of the higher anti-MOG IgG levels in BN rats as compared with BN.DA-*Eae5* rats would be a consumption of circulating MOG-specific Abs in the more diseased BN.DA-*Eae5* rats, displaying more inflammation in the CNS with an opened blood-brain barrier allowing passage of MOG-specific Abs. We have observed similar phenomena in drug-treated MOG-EAE rats, where those with no or mild disease displayed higher anti-MOG IgG levels than the vehicle-treated, severely diseased rats (44).

Detailed positioning of the effect would require extensive breeding with a selection of recombinants within a congenic region. This is not easily achieved, as the BN strain is a poor breeder. High-resolution mapping of *Eae5* was therefore performed using the advanced intercross line G7 (DA × PVG.1AV1). With this approach we were able to map *Eae5* to a ~1.3-Mb region. As compared with the outcome using microsatellite markers, adding specific SNP markers in exons 4 and 6 in the *Ncf-1* gene, respectively (18), improved the level of significance 10-fold (Fig. 4). This result may reflect either linkage to *Ncf-1* or to nearby genes. DA alleles confer an increase in EAE incidence and higher means of maximum EAE score, cumulative EAE score, and duration of disease in a recessive fashion. The confidence interval encompasses seven confirmed genes, including *Ncf-1*, and 13 unconfirmed genes (Table II). Of these genes, only *Ncf-1* was previously sequenced and known to be polymorphic in exon 6 between DA, BN, and PVG.1AV1. Codon 153 in *Ncf-1* exon 6 is ATG in DA and ACG in BN and PVG.1AV1 (M153T substitution) rats (Ref. 40 and present paper). The DA genotype is linked to a low oxidative burst and the BN genotype to a high oxidative burst, respectively. The role of *Ncf-1* in MOG-EAE regulation has recently been demonstrated in mice and is related to the function of APCs and the processing and presentation of Ags (38). We here present congenic BN.DA-*Eae5* data, AIL data, and the sequence polymorphism data, all of which together strongly suggest that *Ncf-1* might also explain the regulatory effect of *Eae5* in rat MOG-EAE. Furthermore, we here use the DA strain for MOG-EAE induction, which is considered to be a model for encephalomyelitis more closely resembling human MS than many other rodent models in regard to disease course, demyelination, and axonal damage (19–21).

We speculate that the present genetic evidence suggesting a role of *Ncf-1* in EAE may shed light on the role of NO in EAE. Some studies suggest detrimental effects and others a protective role of NO in CNS inflammatory diseases (45) (46). NO affects nerve fibers and nerve conduction negatively (47) (48). Paradoxically, resistant PVG rats develop full-blown EAE if NO production is blocked (49). The M153T substitution in *Ncf-1* in the resistant strains (BN, E3, and PVG.1AV1) results in a high oxidative burst as mentioned previously. The superoxide produced during the oxidative burst can react with NO, producing high levels of the very reactive and toxic molecule peroxynitrite. It has been suggested that peroxynitrite may have a potential role in the pathogenesis of clinical EAE and demyelinating lesions (reviewed in Refs. 50 and 51). In contrast, a more suitable hypothesis correlating with our results would be that peroxynitrite dampens autoaggressive anti-MOG immune responses. This would explain part of the EAE resistance in PVG rats, which potentially have a higher oxidative burst as well as higher levels of peroxynitrite as compared with DA rats. If so, DA rats would not develop more severe EAE with NO blocking because they normally display a low oxidative burst. Instead, we would expect a milder clinical EAE course due to the inhibition of the toxic NO effects on the nervous system. This indeed seems to be the case in DA rat MOG-EAE (52). Consequently, the outcome of NO being blocked would in part depend on the *Ncf-1* genotype.

Although the relevance of synonymous changes, SNPs in UTRs, and expression differences in other tissues and time points cannot be excluded, our data suggest *Ncf-1* and *CLDN4* as the strongest candidates in *Eae5*. These are tightly linked and, therefore, difficult to separate. Congenic strains with recombinations between *Ncf-1*

and *CLDN4* will, however, be established in the DA and PVG.1AV1 strain combination to enable a genetic dissection of this region and to confirm whether there are several genes acting jointly with an influence on EAE as was recently demonstrated for *Eae18* (53). Interestingly, *CLDN4* contained one polymorphism that resulted in a K191E change, segregating between EAE-susceptible and EAE-resistant rat strains (Fig. 6*a*. and Table III). Moreover, there were distinct differences in expression in both naive and MOG-immunized DA rats as compared with PVG.1AV1 and BN rats in several tissues of relevance for EAE. The claudins belong to a family of integral membrane tight junction proteins and comprise >20 members that are of importance for the formation of tight junction strands (54) (Ensembl). Claudin expression is considered to be tissue specific, even if previous data presented has shown the difficulties of accurately defining specificity due to cross-reactivity (27). Our data, however, suggest *CLDN4* as a very interesting candidate for disease regulation, controlling the influx of inflammatory cells into the target organ. Furthermore, previous studies in mice have demonstrated a selective loss of *Cldn3* in the blood-brain barrier during EAE (27). Looking at the pathological differences, the major feature is that BN rats have a low degree of inflammation but quite extensive demyelination, whereas the DA rats display both inflammation and demyelination. One possible explanation for this finding is that in BN rats the disease develops in a similar way as in DA rats in the early stage of disease, but the BN rats recover without further disease progression. In contrast, in DA rats early disease may be a bit milder, but the disease progresses and the rats have extensive inflammation and demyelination until the stage at which they are sampled. A possible explanation for such a scenario could be that the given *CLDN4* genotype is also of importance in the integrity of the blood-brain barrier, leading to a more rapid repair and, thus, inhibition of disease progression in BN rats.

In addition, the syntenic human region on 7q11.23 contains claudin-3 and claudin-4, and the syntenic mouse region on chromosome 5 contains claudin-3, claudin-4, and claudin-13. The expression pattern of claudins is nonrandomly distributed (55). The literature on claudin expression in different tissues and interspecies differences is, however, not well defined. Accordingly, we therefore cannot exclude any of these claudins. Instead, we believe that these results suggest that *CLDN4* in this case is of relevance in EAE regulation in rat and that specific claudins most probably are involved in MS pathogenesis (B. Engelhardt, personal communication). Furthermore, the *Eae5* region is syntenic to the human 7q11.23 region that was previously identified in a linkage analysis performed on MS material (26). This finding strengthens the comparative mapping approach that we have applied and present in this work. More importantly, this study suggests claudins, as a protein family, to be strong candidate genes for EAE and MS disease regulation. Accordingly, association studies on several claudins are currently underway in our laboratory and will be tested in MS material and healthy controls and in several other inflammatory diseases.

In conclusion, we demonstrate in this work a regulatory effect of *Eae5* on MOG-EAE using congenic strains and we fine map these effects to a ~1.3-Mb region containing *Ncf-1*, a gene with reported effects in experimental arthritis and encephalomyelitis. Thus, if *Ncf-1* is indeed the gene that regulates MOG-EAE, as the evidence strongly suggests, it would be an example of a shared gene between different organ-specific inflammatory diseases. Moreover, we here confirm the relevance of *Ncf-1* in inflammatory disease in the rat. *Ncf-1* is duplicated in the human genome, which makes the interpretation of genotyping data and, thus, association studies in humans difficult. In this case we believe that the use of inbred and established congenic rat strains will be of major importance. Phenotyping the function of *Ncf-1* in inbred and congenic strains will help us to elucidate the role of *Ncf-1*. Subsequently, this line of research could be addressed in humans and possibly lead to the establishment of diagnostic assays and/or tools that can be used in the clinics to diagnose rheumatoid arthritis and MS patients. Furthermore, our sequence and expression data suggest *CLDN4* as a candidate gene operating in encephalomyelitis. Future work will, however, resolve the question of whether *Eae5* contains several EAE-regulatory genes closely linked to *Ncf-1*. This question suggests that studies should be undertaken to assess whether this gene or genes in the same pathway are of importance for human MS in addition to rheumatoid arthritis.

Acknowledgments

We thank Assoc. Prof. Robert Harris for linguistic advice and Prof. Britta Engelhardt for personal communication.

Disclosures

The authors have no financial conflict of interest.

References

1. Sadovnick, A. D., P. A. Baird, and R. H. Ward. 1988. Multiple sclerosis: updated risks for relatives. *Am. J. Med. Genet.* 29: 533–541.
2. Svejgaard, A., C. Jersild, L. S. Nielsen, and W. F. Bodmer. 1974. HL-A antigens and disease: statistical and genetical considerations. *Tissue Antigens* 4: 95–105.
3. Jersild, C., B. Dupont, A. Svejgaard, P. J. Platz, K. A. Ciongoli, and T. Fog. 1975. Proceedings: Genetic factors in multiple sclerosis: the major histocompatibility system (HL-A) and immunity. *Neurology* 25: 488–489.
4. Masterman, T., A. Ligers, T. Olsson, M. Andersson, O. Olerup, and J. Hillert. 2000. HLA-DR15 is associated with lower age at onset in multiple sclerosis. *Ann. Neurol.* 48: 211–219.
5. Olerup, O., and J. Hillert. 1991. HLA class II-associated genetic susceptibility in multiple sclerosis: a critical evaluation. *Tissue Antigens* 38: 1–15.
6. Sundvall, M., J. Jirholt, H. T. Yang, L. Jansson, A. Engstrom, U. Pettersson, and R. Holmdahl. 1995. Identification of murine loci associated with susceptibility to chronic experimental autoimmune encephalomyelitis. *Nat. Genet.* 10: 313–317.
7. Baker, D., O. A. Rosenwasser, J. K. O'Neill, and J. L. Turk. 1995. Genetic analysis of experimental allergic encephalomyelitis in mice. *J. Immunol.* 155: 4046–4051.
8. Butterfield, R. J., J. D. Sudweeks, E. P. Blankenhorn, R. Korngold, J. C. Marini, J. A. Todd, R. J. Roper, and C. Teuscher. 1998. New genetic loci that control susceptibility and symptoms of experimental allergic encephalomyelitis in inbred mice. *J. Immunol.* 161: 1860–1867.
9. Dahlman, I., L. Jacobsson, A. Glaser, J. C. Lorentzen, M. Andersson, H. Luthman, and T. Olsson. 1999. Genome-wide linkage analysis of chronic relapsing experimental autoimmune encephalomyelitis in the rat identifies a major susceptibility locus on chromosome 9. *J. Immunol.* 162: 2581–2588.
10. Dahlman, I., E. Wallstrom, R. Weissert, M. Storch, B. Kornek, L. Jacobsson, C. Linington, H. Luthman, H. Lassmann, and T. Olsson. 1999. Linkage analysis of myelin oligodendrocyte glycoprotein-induced experimental autoimmune encephalomyelitis in the rat identifies a locus controlling demyelination on chromosome 18. *Hum. Mol. Genet.* 8: 2183–2190.
11. Roth, M. P., C. Viratelle, L. Dolbois, M. Delverdier, N. Borot, L. Pelletier, P. Druet, M. Clanet, and H. Coppin. 1999. A genome-wide search identifies two susceptibility loci for experimental autoimmune encephalomyelitis on rat chromosomes 4 and 10. *J. Immunol.* 162: 1917–1922.
12. Encinas, J. A., and V. K. Kuchroo. 2000. Mapping and identification of autoimmunity genes. *Curr. Opin. Immunol.* 12: 691–697.
13. Encinas, J. A., M. B. Lees, R. A. Sobel, C. Symonowicz, H. L. Weiner, C. E. Seidman, J. G. Seidman, and V. K. Kuchroo. 2001. Identification of genetic loci associated with paralysis, inflammation and weight loss in mouse experimental autoimmune encephalomyelitis. *Int. Immunol.* 13: 257–264.
14. Bergsteinsdottir, K., H. T. Yang, U. Pettersson, and R. Holmdahl. 2000. Evidence for common autoimmune disease genes controlling onset, severity, and chronicity based on experimental models for multiple sclerosis and rheumatoid arthritis. *J. Immunol.* 164: 1564–1568.
15. Becanovic, K., E. Wallstrom, B. Kornek, A. Glaser, K. W. Broman, I. Dahlman, P. Olofsson, R. Holmdahl, H. Luthman, H. Lassmann, and T. Olsson. 2003. New loci regulating rat myelin oligodendrocyte glycoprotein-induced experimental autoimmune encephalomyelitis. *J. Immunol.* 170: 1062–1069.
16. Darvasi, A., and M. Soller. 1995. Advanced intercross lines, an experimental population for fine genetic mapping. *Genetics* 141: 1199–1207.
17. Vingsbo-Lundberg, C., N. Nordquist, P. Olofsson, M. Sundvall, T. Saxne, U. Pettersson, and R. Holmdahl. 1998. Genetic control of arthritis onset, severity and chronicity in a model for rheumatoid arthritis in rats. *Nat. Genet.* 20: 401–404.
18. Olofsson, P., J. Holmberg, J. Tordsson, S. Lu, B. Akerstrom, and R. Holmdahl. 2003. Positional identification of *Ncf1* as a gene that regulates arthritis severity in rats. *Nat. Genet.* 33: 25–32.

19. Weissert, R., E. Wallstrom, M. K. Storch, A. Stefferl, J. Lorentzen, H. Lassmann, C. Linington, and T. Olsson. 1998. MHC haplotype-dependent regulation of MOG-induced EAE in rats. *J. Clin. Invest.* 102: 1265–1273.
20. Storch, M. K., A. Stefferl, U. Brehm, R. Weissert, E. Wallstrom, M. Kerschensteiner, T. Olsson, C. Linington, and H. Lassmann. 1998. Autoimmunity to myelin oligodendrocyte glycoprotein in rats mimics the spectrum of multiple sclerosis pathology. *Brain Pathol.* 8: 681–694.
21. Kornek, B., M. K. Storch, R. Weissert, E. Wallstrom, A. Stefferl, T. Olsson, C. Linington, M. Schmidbauer, and H. Lassmann. 2000. Multiple sclerosis and chronic autoimmune encephalomyelitis: a comparative quantitative study of axonal injury in active, inactive, and remyelinated lesions. *Am. J. Pathol.* 157: 267–276.
22. Lyons, J. A., M. San, M. P. Happ, and A. H. Cross. 1999. B cells are critical to induction of experimental allergic encephalomyelitis by protein but not by a short encephalitogenic peptide. *Eur. J. Immunol.* 29: 3432–3439.
23. Lyons, J. A., M. J. Ramsbottom, and A. H. Cross. 2002. Critical role of antigen-specific antibody in experimental autoimmune encephalomyelitis induced by recombinant myelin oligodendrocyte glycoprotein. *Eur. J. Immunol.* 32: 1905–1913.
24. Linington, C., M. Bradl, H. Lassmann, C. Brunner, and K. Vass. 1988. Augmentation of demyelination in rat acute allergic encephalomyelitis by circulating mouse monoclonal antibodies directed against a myelin/oligodendrocyte glycoprotein. *Am. J. Pathol.* 130: 443–454.
25. Weissert, R., K. L. de Graaf, M. K. Storch, S. Barth, C. Linington, H. Lassmann, and T. Olsson. 2001. MHC class II-regulated central nervous system autoaggression and T cell responses in peripheral lymphoid tissues are dissociated in myelin oligodendrocyte glycoprotein-induced experimental autoimmune encephalomyelitis. *J. Immunol.* 166: 7588–7599.
26. Haines, J. L., M. Ter-Minassian, A. Bazyk, J. F. Gusella, D. J. Kim, H. Terwedow, M. A. Pericak-Vance, J. B. Rimmler, C. S. Haynes, A. D. Roses, et al. 1996. A complete genomic screen for multiple sclerosis underscores a role for the major histocompatability complex. *Nat. Genet.* 13: 469–471.
27. Wolburg, H., K. Wolburg-Buchholz, J. Kraus, G. Rascher-Eggstein, S. Liebner, S. Hamm, F. Duffner, E. H. Grote, W. Risau, and B. Engelhardt. 2003. Localization of claudin-3 in tight junctions of the blood-brain barrier is selectively lost during experimental autoimmune encephalomyelitis and human glioblastoma multiforme. *Acta Neuropathol.* 105: 586–592.
28. Wakeland, E., L. Morel, K. Achey, M. Yui, and J. Longmate. 1997. Speed congenics: a classic technique in the fast lane (relatively speaking). *Immunol. Today* 18: 472–477.
29. Amor, S., N. Groome, C. Linington, M. M. Morris, K. Dornmair, M. V. Gardinier, J. M. Matthieu, and D. Baker. 1994. Identification of epitopes of myelin oligodendrocyte glycoprotein for the induction of experimental allergic encephalomyelitis in SJL and Biozzi AB/H mice. *J. Immunol.* 153: 4349–4356.
30. Laird, P. W., A. Zijderveld, K. Linders, M. A. Rudnicki, R. Jaenisch, and A. Berns. 1991. Simplified mammalian DNA isolation procedure. *Nucleic Acids Res.* 19: 4293.
31. Jacob, H. J., D. M. Brown, R. K. Bunker, M. J. Daly, V. J. Dzau, A. Goodman, G. Koike, V. Kren, T. Kurtz, A. Lernmark, et al. 1995. A genetic linkage map of the laboratory rat, *Rattus norvegicus*. *Nat. Genet.* 9: 63–69.
32. Lander, E. S., P. Green, J. Abrahamson, A. Barlow, M. J. Daly, S. E. Lincoln, and L. Newburg. 1987. MAPMAKER: an interactive computer package for constructing primary genetic linkage maps of experimental and natural populations. *Genomics* 1: 174–181.
33. Broman, K. W., H. Wu, S. Sen, and G. A. Churchill. 2003. R/qtl: QTL mapping in experimental crosses. *Bioinformatics* 19: 889–890.
34. Doerge, R. W., and G. A. Churchill. 1996. Permutation tests for multiple loci affecting a quantitative character. *Genetics* 142: 285–294.
35. Churchill, G. A., and R. W. Doerge. 1994. Empirical threshold values for quantitative trait mapping. *Genetics* 138: 963–971.
36. Gracie, J. A., and J. A. Bradley. 1996. Interleukin-12 induces interferon-γ-dependent switching of IgG alloantibody subclass. *Eur. J. Immunol.* 26: 1217–1221.
37. Mussener, A., J. C. Lorentzen, S. Kleinau, and L. Klareskog. 1997. Altered Th1/Th2 balance associated with non-major histocompatibility complex genes in collagen-induced arthritis in resistant and non-resistant rat strains. *Eur. J. Immunol.* 27: 695–699.
38. Hultqvist, M., P. Olofsson, J. Holmberg, B. T. Backstrom, J. Tordsson, and R. Holmdahl. 2004. Enhanced autoimmunity, arthritis, and encephalomyelitis in mice with a reduced oxidative burst due to a mutation in the Ncf1 gene. *Proc. Natl. Acad. Sci. USA* 101: 12646–12651.
39. Lander, E. S., and D. Botstein. 1989. Mapping Mendelian factors underlying quantitative traits using RFLP linkage maps. *Genetics* 121: 185–199.
40. Olofsson, P., and R. Holmdahl. 2003. Positional cloning of Ncf1: a piece in the puzzle of arthritis genetics. *Scand. J. Immunol.* 58: 155–164.
41. Wolburg, H., K. Wolburg-Buchholz, S. Liebner, and B. Engelhardt. 2001. Claudin-1, claudin-2 and claudin-11 are present in tight junctions of choroid plexus epithelium of the mouse. *Neurosci. Lett.* 307: 77–80.
42. Virgintino, D., M. Errede, D. Robertson, C. Capobianco, F. Girolamo, A. Vimercati, M. Bertossi, and L. Roncali. 2004. Immunolocalization of tight junction proteins in the adult and developing human brain. *Histochem. Cell Biol.* 122: 51–59.
43. Wilcox, E. R., Q. L. Burton, S. Naz, S. Riazuddin, T. N. Smith, B. Ploplis, I. Belyantseva, T. Ben-Yosef, N. A. Liburd, R. J. Morell, et al. 2001. Mutations in the gene encoding tight junction claudin-14 cause autosomal recessive deafness DFNB29. *Cell* 104: 165–172.
44. Eltayeb, S., D. Sunnemark, A. L. Berg, G. Nordvall, A. Malmberg, H. Lassmann, E. Wallstrom, T. Olsson, and A. Ericsson-Dahlstrand. 2003. Effector stage CC chemokine receptor-1 selective antagonism reduces multiple sclerosis-like rat disease. *J. Neuroimmunol.* 142: 75–85.
45. Smith, K. J., and H. Lassmann. 2002. The role of nitric oxide in multiple sclerosis. *Lancet Neurol.* 1: 232–241.
46. Smith, K. J., R. Kapoor, and P. A. Felts. 1999. Demyelination: the role of reactive oxygen and nitrogen species. *Brain Pathol.* 9: 69–92.
47. Redford, E. J., R. Kapoor, and K. J. Smith. 1997. Nitric oxide donors reversibly block axonal conduction: demyelinated axons are especially susceptible. *Brain* 120: 2149–2157.
48. Smith, K. J., and S. M. Hall. 2001. Factors directly affecting impulse transmission in inflammatory demyelinating disease: recent advances in our understanding. *Curr. Opin. Neurol.* 14: 289–298.
49. Cowden, W. B., F. A. Cullen, M. A. Staykova, and D. O. Willenborg. 1998. Nitric oxide is a potential down-regulating molecule in autoimmune disease: inhibition of nitric oxide production renders PVG rats highly susceptible to EAE. *J. Neuroimmunol.* 88: 1–8.
50. Torreilles, F., S. Salman-Tabcheh, M. Guerin, and J. Torreilles. 1999. Neurodegenerative disorders: the role of peroxynitrite. *Brain Res. Brain Res. Rev.* 30: 153–163.
51. Cross, A. H., M. San, M. K. Stern, R. M. Keeling, D. Salvemini, and T. P. Misko. 2000. A catalyst of peroxynitrite decomposition inhibits murine experimental autoimmune encephalomyelitis. *J. Neuroimmunol.* 107: 21–28.
52. Danilov, A. I., M. Jagodic, N. P. Wiklund, T. Olsson, and L. Brundin. 2005. Effects of long term NOS inhibition on disease and the immune system in MOG-induced EAE. *Nitric Oxide* 13: 188–195.
53. Jagodic, M., K. Becanovic, J. R. Sheng, X. Wu, L. Backdahl, J. C. Lorentzen, E. Wallstrom, and T. Olsson. 2004. An advanced intercross line resolves Eae18 into two narrow quantitative trait loci syntenic to multiple sclerosis candidate loci. *J. Immunol.* 173: 1366–1373.
54. Morita, K., M. Furuse, K. Fujimoto, and S. Tsukita. 1999. Claudin multigene family encoding four-transmembrane domain protein components of tight junction strands. *Proc. Natl. Acad. Sci. USA* 96: 511–516.
55. Engelhardt, B. 2003. Development of the blood-brain barrier. *Cell Tissue Res.* 314: 119–129.